

# Changes in the Silanol Protonation State Measured In Situ at the Silica–Aqueous Interface

Matthew A. Brown,<sup>\*,†</sup> Thomas Huthwelker,<sup>‡</sup> Amaia Belouqui Redondo,<sup>†</sup> Markus Janousch,<sup>‡</sup> Manfred Faubel,<sup>§</sup> Christopher A. Arrell,<sup>⊥</sup> Mariateresa Scarongella,<sup>⊥</sup> Majed Chergui,<sup>⊥</sup> and Jeroen A. van Bokhoven<sup>†,‡</sup>

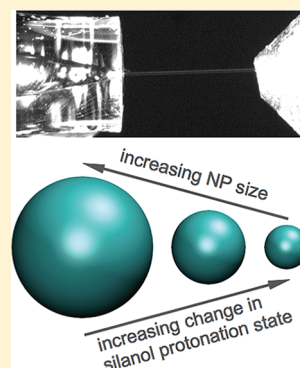
<sup>†</sup>Institute for Chemical and Bioengineering, ETH Zürich, CH-8093 Zürich, Switzerland

<sup>‡</sup>Swiss Light Source, Paul Scherrer Institute, CH-5232 Villigen PSI, Switzerland

<sup>§</sup>Max Planck Institute for Dynamics and Self-Organization, D-37073 Göttingen, Germany

<sup>⊥</sup>Laboratory for Ultrafast Spectroscopy, EPFL, CH-1015 Lausanne, Switzerland

**ABSTRACT:** Recent nanomedical applications have again highlighted the significance of silica surface chemistry in solution. Here, we report in situ electronic structure measurements at the silica–aqueous interface as a function of pH for nanoparticles (NPs) of 7, 12, and 22 nm using a liquid microjet in combination with synchrotron radiation. The Si K-edge X-ray absorption near-edge spectroscopy (XANES) spectra reveal a change in shape of the Si 1s  $\rightarrow$  t<sub>2</sub> (Si 2p–3s) absorption brought about by changes in the silanol protonation state at the interface of the NPs as a result of changes in solution pH. Our results are consistent with the number of silanol groups changing the protonation state being inversely correlated with the SiO<sub>2</sub> NP size. The importance of in situ studies is also demonstrated by comparing the XANES spectra of aqueous 7 nm SiO<sub>2</sub> with the same dehydrated sample in vacuum.



**SECTION:** Surfaces, Interfaces, Catalysis

The solid–liquid interface is one of the most important areas of current research because of its prevalence in fields as diverse as catalysis and electrochemistry to environmental and biological sciences. However, because two condensed phases are involved, this interface is difficult to interrogate quantitatively at a molecular level. As such, gaining molecular-level insight of the solid–liquid interface is considered the next significant challenge for the surface science community<sup>1</sup> who has already established molecular-level probes for the solid–vacuum/gas interface.<sup>2</sup>

The solid–liquid interface of silicon nanoparticles (NPs) has recently received renewed interest for its biocompatibility<sup>3</sup> and complete biodegradability<sup>4</sup> in nanomedical applications.<sup>5,6</sup> The potential broad benefits of silicon NPs in the field of nanomedicine has in turn highlighted the significance of being able to both control the surface chemistry of silicon NPs in aqueous solution and provide a molecular-level description of the interface structure.<sup>6</sup>

A variety of surface treatments have been developed to modify the surface charge of silica NPs as the protonation state of the silanol groups at the silica–aqueous interface is believed to largely control its chemistry.<sup>7</sup> Positive or negative charges can be created on the silica NP surface by changing the pH in aqueous solution. However, because of the relatively narrow pH range for which traditional potentiometric acid–base surface titrations work,<sup>8</sup> the unambiguous establishment of the isoelectric point (IEP) of silica remains debated (~1.8–4.0).

At pH units below the IEP of silica, the NP surface has an overall net positive charge and contains protonated silanol groups,  $\equiv\text{Si}-\text{OH}_2^+$ , in addition to the majority species,  $\equiv\text{Si}-\text{O}-\text{Si}\equiv$  and  $\equiv\text{Si}-\text{OH}$ , that exist at all pHs.<sup>7,8</sup> At pH units above the IEP, the surface has an overall net negative charge and contains deprotonated silanol groups,  $\equiv\text{Si}-\text{O}^-$ .<sup>7,9</sup>

A molecular-level understanding of the pH-dependent silica–aqueous interface is far from complete and limited by the number of in situ analytical techniques that can probe the solid–liquid interface at the molecular level.<sup>1</sup> As a result, most of the electronic structure information gained about the silica–aqueous interface, which is then often used to develop physical models of speciation at the interface, has been obtained with ex situ core-level electron spectroscopies on samples that have either been fast-frozen,<sup>10–12</sup> frozen wet pastes,<sup>13</sup> or dehydrated<sup>9</sup> to gain vacuum compatibility. The effect of these sample pretreatments to the silica–aqueous interface often questions the validity of such results for applications where the silica interface is in constant contact with an aqueous environment.

In this Letter, we provide a description of the physical and electronic structures of silica NPs as a function of size and pH in aqueous solution. Our in situ Si K-edge X-ray absorption

**Received:** November 21, 2011

**Accepted:** January 3, 2012

**Published:** January 3, 2012

near-edge spectroscopy (XANES) measurements probe the electronic structure of the silica–aqueous interface and reveal a NP size dependence on the fraction of surface silanol groups that change the protonation state as a result of changes in solution pH. The experiment also highlights XANES as a molecular-level analytical tool capable of interrogating the solid–liquid interface at extreme pH values where conventional acid–base titrations fail.

Our experiments used a 35  $\mu\text{m}$  liquid jet<sup>14–16</sup> operating at 279 K to deliver a 3 wt % aqueous colloidal silica suspension.<sup>17</sup> Suspensions were prepared at pH 0.3, by the addition of concentrated HCl, and at pH 10.0, which was the native pH obtained by diluting the stock Ludox<sup>17</sup> suspension. The stability of the colloidal suspensions is at a maximum at these extreme pH values, which allows for statistical averaging of the spectra over the course of several hours. By contrast, intermediate pH values result in limited stability of the colloidal suspensions and prevent a thorough investigation of their electronic structure at the present time. The net charge of the silica NPs was determined to be  $+25.5 \pm 12.2$  and  $-55.5 \pm 6.6$  mV at pH 0.3 and 10.0, respectively, by Zeta potential measurements.

Figure 1 shows the normalized Si K-edge fluorescence spectra recorded for a 3 wt % aqueous colloidal 7 nm silica

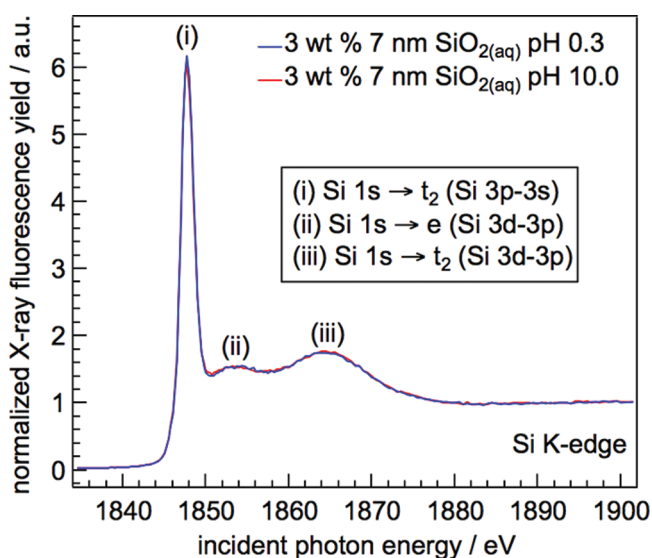


**Figure 1.** Normalized silicon fluorescence yield K-edge X-ray absorption spectra from aqueous 3 wt % colloidal suspensions of 7 nm  $\text{SiO}_2$  NPs at pH 0.3 (blue) and 10.0 (red). The assignments of the three distinct absorptions labeled in the spectra are shown in the inset. Spectra have been normalized to the intensity at 1900 eV.

suspension at pH 0.3 and 10.0. Each spectrum represents the average of 30 spectra and has been normalized to the intensity at 1900 eV. There are three distinct absorptions in the spectra that are in qualitative agreement with previous XANES measurements of amorphous silica (solid–vacuum interface) recorded in vacuum.<sup>18,19</sup> On the basis of the tetrahedral symmetry of amorphous silica,<sup>20</sup> the assignments of the three absorptions are (i)  $\text{Si } 1s \rightarrow t_2$  ( $\text{Si } 3p-3s$ ) at 1847.7 eV, (ii)  $\text{Si } 1s \rightarrow e$  ( $\text{Si } 3d-3p$ ) at 1853.5 eV, and (iii)  $\text{Si } 1s \rightarrow t_2$  ( $\text{Si } 3d-3p$ ) at 1864.5 eV. As expected with amorphous materials that lack a periodic ordering, the multiple scattering peaks of crystalline  $\alpha$  silica at  $\sim 1850.7$  and  $\sim 1857.4$  eV are not seen.<sup>19</sup>

Figure 2a gives the difference spectrum that results from the two spectra of Figure 1. The ordinate represents the percent

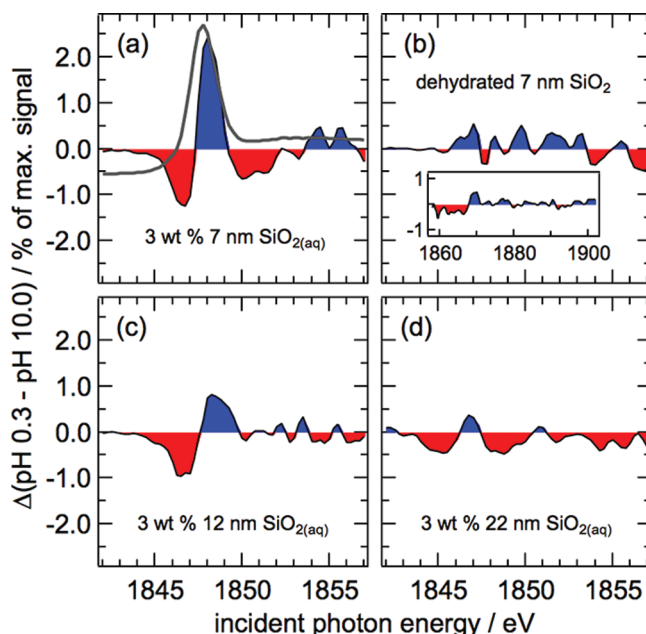


**Figure 2.** (a) Difference curve of the spectra shown in Figure 1. The spectrum at pH 10.0 from Figure 1 is also shown in gray as a visual guide to mark the position of the edge (arbitrary scaling). (b) Similar difference curve for dehydrated 7 nm  $\text{SiO}_2$  recorded after depositing the liquid samples onto a copper plate and removing water under a controlled  $\text{N}_2$  gas flow. The spectra of dehydrated 7 nm  $\text{SiO}_2$  were collected in  $10^{-5}$  mbar vacuum. The inset of (b) shows the difference spectrum of region (iii) and is used to set the statistical fluctuation of the experiment to below 0.3%. Difference curve for aqueous 3 wt % colloidal suspensions of (c) 12 and (d) 22 nm  $\text{SiO}_2$  NPs. For all samples, only regions (i) and (ii) (assignment of Figure 1) are shown.

deviation from the maximum-recorded signal intensity of Figure 1 (i.e.,  $[(\text{pH } 0.3 - \text{pH } 10.0)/\text{max intensity of pH } 10.0] \times 100\%$ ). The spectrum of pH 10.0 of Figure 1 is also plotted in Figure 2a as a visual guide to mark the position of the edge. Similar difference spectra are shown in Figure 2c and d for aqueous 3 wt % colloidal suspensions of 12 and 22 nm  $\text{SiO}_2$ , respectively. The difference spectrum of each NP size shares a similar structure but differs in amplitude. All difference spectra show a region of negative difference below the edge maximum with a near-zero difference centered on the edge maximum. The maximum positive difference is centered  $\sim 0.3$  eV above the edge maximum. Finally, another region of negative difference is centered at an energy  $\sim 3$  eV above the edge maximum. The difference spectra in region (iii) and to higher energies exhibit only minor deviations from zero that are within the statistical fluctuations of the experiment (inset of Figure 2b). This region also serves to establish the limitations of the present study and to set the statistical fluctuations of the experiment to below 0.3%. The integral of the difference spectra for 7 and 12 nm silica particles is near zero, as derived from Figure 2a and c, which strongly suggests that there is no net change in the density of states (DOS) of the system, but instead, the difference observed originates from a change in shape of the two spectra centered around the maximum absorption.

To emphasize the importance of in situ measurements at the silica–aqueous interface, dehydrated samples of 7 nm  $\text{SiO}_2$  were prepared by depositing the liquid samples onto a copper substrate and subsequently removing the liquid content under a controlled  $\text{N}_2$  gas flow. The Si K-edge XANES spectra of the solid dehydrated samples were then recorded in  $10^{-5}$  mbar vacuum. The difference spectrum obtained from the solid samples measured under vacuum is shown in Figure 2b.

Si K-edge fluorescence XANES is generally considered a bulk electronic structure probe of the unoccupied Si p-like DOS of silicon-containing compounds.<sup>21</sup> The signal intensity or fluorescence yield of such an experiment is a direct product of the unoccupied p-like DOS of the absorbing Si atom and the number of absorbing Si atoms in the system. Because the present NPs of study are nonporous,<sup>17</sup> differences in surface potential (charge) resulting from changes in pH are expected to affect only the outermost surface layer of the NP that is in direct contact with aqueous solution.<sup>22</sup> As a result, the majority intensity of the XANES spectra of Figure 1 is unaffected by changes in solution pH as the signal originates from the bulk of the NP. The difference spectra of Figure 2 result from changes in Si electronic structures brought about by changes in the protonation state of the silanol groups, uniquely at the silica–aqueous interface of these NPs. In addition, changes in solution pH are not expected to affect the size of the silica NP, and therefore, a ripening effect can also be ruled out as a possible origin to the spectral differences.<sup>23</sup>

The absolute Si concentration at the interface relative to the total Si content of the NP is difficult to quantitatively determine because the microscopic structure of the amorphous NP is poorly defined. Qualitative estimates are however possible assuming a Si–O bond distance of 1.6 Å.<sup>24</sup> Combining this approximation with the number of silanol groups per unit surface area of silica<sup>7</sup> would provide an estimate of the upper limit of the signal intensity originating from the surface Si atoms of the NP that contain silanol groups,  $\equiv\text{Si}-\text{OH}$ , in aqueous solution when using a probe such as Si K-edge XANES that is not inherently surface-sensitive. Such an estimate assumes that the total area of the DOS remains constant and only a change in shape occurs as a result of protonation state. This assumption is corroborated by the observation that the integral of the difference spectra shown in Figure 2 is zero, and therefore, the total DOS can be inferred to be constant for this system. For a 7 nm diameter NP, the volume of an outer shell of 1.6 Å thickness is  $\sim 13\%$  of the total NP volume. Using a silanol number density of  $50\%$ ,<sup>7</sup> we would expect the maximum signal contribution originating from surface Si atoms that contain silanol groups in the Si K-edge XANES spectrum as the pH is varied to be  $\sim 6.5\%$  of the total recorded signal intensity. By comparison, a 2.4% intensity difference is recorded in the experiment (Figure 2a) ( $\sim 37\%$  of the expected maximum signal intensity). For 12 and 22 nm NPs, the outer 1.6 Å monolayer contains, respectively,  $\sim 7.8$  and  $\sim 4.3\%$  Si relative to total Si content of the NP, or 3.9 and 2.2% when accounting for the silanol number density. Intensity differences of 0.8 ( $\sim 28\%$  of maximum signal) and 0.5% ( $\sim 23\%$  of maximum signal) are recorded in the experiment for 12 and 22 nm NPs, respectively (Figure 2c and d).

Because the silanol number density is believed to be constant with silica surface area,<sup>7</sup> the results of the present study would indicate that for smaller NPs of  $\text{SiO}_2$ , there is a larger fraction of surface silanols that change the protonation state with changes in solution pH. Changes in local pH at the liquid–vapor

interface are not believed to influence the results of the present study for several reasons. First, the debate in the literature related to either increased acidity ( $\text{H}_3\text{O}^+$ ) or basicity ( $\text{OH}^-$ ) at the liquid–vapor interface is believed to be localized to the outermost few layers in solution, whereas the NPs of this study have a diameter on the order of (for the smallest NPs) greater than  $\sim 20$  layers of water. Second, the spatial distribution of the NPs at the liquid–vapor interface, as inferred by surface tension methods, is believed to be constant in the 7–22 nm size regime,<sup>25</sup> and we therefore expect a roughly constant distribution of the NPs at the liquid–vapor interface irrespective of NP size. With these factors taken into account, the NP size dependence shown in this study may help shed light on why a broad range of values are currently reported in the literature based on dissolution rates and surface titrations for the fraction of surface silanols that change the protonation state with changes in solution pH.<sup>8</sup>

The importance of in situ measurements at the silica–aqueous interface is evident by comparing Figure 2a and b. While these spectra are difficult to compare on a quantitative level because the dehydration process results in a ripening or agglomeration of the silica NP into micrometer-sized particles (Figure 3), a qualitative difference is prominent. The difference

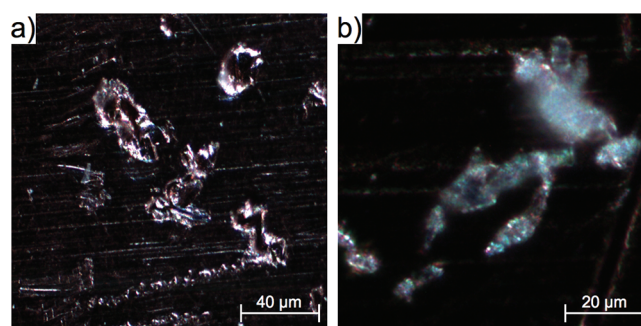


**Figure 3.** Light microscope images of dehydrated 7 nm  $\text{SiO}_2$  NPs at (a) pH 0.3 and (b) pH 10.0. The liquid samples were deposited onto a copper plate and dehydrated under a controlled flow of  $\text{N}_2$  gas. XANES fluorescence spectra were collected using the same parameters as those for the liquid samples in a vacuum of  $10^{-5}$  mbar.

spectrum of dehydrated  $\text{SiO}_2$  shows a significantly reduced intensity (within the statistical fluctuations of the experiment) and no defined structure when compared with the in situ measurement. In particular, with NPs that are known to ripen or agglomerate during dehydration, such as silica,<sup>26</sup> this result brings into question the relevance of ex situ X-ray photoelectron spectroscopy and XANES measurements as appropriate probes of the electronic and physical structures at the solid–liquid interface. This result should be taken into consideration in applications across all disciplines of interfacial science where accurate descriptions of the solid–liquid interface are required.

Electronic structure measurements have been performed in situ at the silica–aqueous interface as a function of pH for NPs of 7, 12, and 22 nm. The Si K-edge XANES spectra reveal a change in shape of the Si  $1s \rightarrow t_2$  (Si  $3p-3s$ ) absorption brought about by changes in the silanol protonation state as a result of changes in solution pH. Our results are consistent with the number of silanol groups changing the protonation state being inversely correlated with  $\text{SiO}_2$  NP size. The fraction of silanol groups at the surface of the smaller NPs that undergo a change



in protonation state as a result of changes in solution pH is higher than that for the larger NPs of this study.

The importance of further developing advanced in situ analytical tools that can probe the solid–liquid interface at a molecular level was also clearly demonstrated by comparing the XANES measurements from aqueous 7 nm SiO<sub>2</sub> with those for dehydrated 7 nm SiO<sub>2</sub>. The noticeable difference in these spectra brings into question the significance of ex situ molecular-level probes to accurately describe the solid–liquid interface.

## ■ EXPERIMENTAL METHODS

**XANES.** Our experiments used a 35  $\mu\text{m}$  liquid jet<sup>14–16</sup> to deliver a 3 wt % aqueous colloidal 7 nm silica suspension.<sup>17</sup> Si K-edge XANES measurements were performed at the Phoenix I beamline of the Swiss Light Source using a double-crystal InSb monochromator with an energy resolution of 0.5 at 1840 eV. Suspensions were prepared at pH 0.3 by the addition of concentrated HCl and at pH 10.0, which was the native pH obtained by diluting the stock Ludox suspension. Suspension pH values were measured using a Metrohm 744 probe. The liquid jet was operated at a flow of  $\sim 0.75$  mL/min and at 279 K in an atmosphere of 500 mbar of He. Total fluorescence yield XANES measurements were performed with the liquid jet, incident X-ray, and fluorescence detector all at 90° angles from each other. Instead of normalizing the recorded fluorescence signal to a current measured upstream of the sample location,  $I_0$ , (as is typically done in XAS), we normalized the fluorescence peak (Si K-edge) to the off-resonant fluorescence emission of the oxygen peak (K-edge), which was simultaneously recorded using the same detector. In addition to accounting for finite fluctuations of beam intensity, this normalization procedure also accounts for deviations in the spatial overlap of the liquid jet (35  $\mu\text{m}$ ) with the incident X-rays (8  $\mu\text{m}$ ) during the course of measurement.

**Zeta Potential.** Zeta potential measurements of 3 wt % 7 nm aqueous colloidal silica suspensions at pH 0.3 and 10.0 were performed with a Malvern Instruments Zetasizer 3000 HS at room temperature. Samples were injected directly into a capillary inside of the measurement cell. Each sample was averaged for  $\sim 30$  min and repeated three times to ensure reproducibility.

## ■ AUTHOR INFORMATION

### Corresponding Author

\*E-mail: matthew.brown@chem.ethz.ch.

## ■ ACKNOWLEDGMENTS

The authors are indebted to R. Wetter and C. Friehe for their technical assistance at the beamline. M.A.B. acknowledges financial support from the ETH Postdoctoral Fellowship Program. This work was partly supported by the NCCR-MUST network of the Swiss NSF. Portions of this work were performed at the X07MB (Phoenix) beamline of the Swiss Light Source at the Paul Scherrer Institute.

## ■ REFERENCES

- (1) Zaera, F. Surface Chemistry at the Liquid/Solid Interface. *Surf. Sci.* **2011**, *605*, 1141–1145.
- (2) Ertl, G. Reactions at Surfaces: From Atoms to Complexity (Nobel Lecture). *Angew. Chem., Int. Ed.* **2008**, *47*, 3524–3535.

- (3) Chin, V.; Collins, B. E.; Sailor, M. J.; Bhatia, S. N. Compatibility of Primary Hepatocytes with Oxidized Nanoporous Silicon. *Adv. Mater.* **2001**, *13*, 1877–1880.
- (4) Canham, L. T. Bioactive Silicon Structure Fabrication through Nanoetching Techniques. *Adv. Mater.* **1995**, *7*, 1033–1037.
- (5) Thomas, J. C.; Pacholski, C.; Sailor, M. J. Delivery of Nanogram Payloads using Magnetic Porous Silicon Microcarriers. *Lab Chip* **2006**, *6*, 782–787.
- (6) Tasciotti, E.; Liu, X. W.; Bhavane, R.; Plant, K.; Leonard, A. D.; Price, B. K.; Cheng, M. M.-C.; Decuzzi, P.; Tour, J. M.; Robertson, F.; Ferrari, M. Mesoporous Silicon Particles as a Multistage Delivery System for Imaging and Therapeutic Applications. *Nat. Nano.* **2008**, *3*, 151–157.
- (7) Zhuravlev, L. T. The Surface Chemistry of Amorphous Silica. Zhuravlev Model. *Colloids Surf., A* **2000**, *173*, 1–38.
- (8) Pokrovsky, O. S.; Golubev, S. V.; Mielczarski, J. A. Kinetic evidences of the existence of positively charged species at the quartz-aqueous solution interface. *J. Colloid Interface Sci.* **2006**, *296*, 189–194.
- (9) Duval, Y.; Mielczarski, J. A.; Pokrovsky, O. S.; Mielczarski, E.; Ehrhardt, J. J. Evidence of the Existence of Three Types of Species at the Quartz–Aqueous Solution Interface at pH 0–10: XPS Surface Group Quantification and Surface Complexation. *J. Phys. Chem. B* **2002**, *106*, 2937–2945.
- (10) Shchukarev, A. XPS at Solid–Liquid Solution Interface. *Adv. Colloid. Interfac.* **2006**, *122*, 149–157.
- (11) Shchukarev, A.; Rosenqvist, J.; Sjöberg, S. XPS Study of the Silica–Water Interface. *J. Electron Spectrosc. Relat. Phenom.* **2004**, *137*, 171–176.
- (12) Shchukarev, A.; Sjöberg, S. XPS with Fast-Frozen Samples: A Renewed Approach to Study the Real Mineral/Solution Interface. *Surf. Sci.* **2005**, *584*, 106–112.
- (13) Cardenas, J. F. Surface Charge of Silica Determined using X-ray Photoelectron Spectroscopy. *Colloids Surf., A* **2005**, *252*, 213–219.
- (14) Brown, M. A.; Faubel, M.; Winter, B. X-Ray Photo- and Resonant Auger-Electron Spectroscopy Studies of Liquid Water and Aqueous Solutions. *Annu. Rep. Prog. Chem., Sect. C: Phys. Chem.* **2008**, *105*, 174–212.
- (15) Winter, B.; Faubel, M. Photoemission from Liquid Aqueous Solutions. *Chem. Rev.* **2006**, *106*, 1176–1211.
- (16) Winter, B. Liquid Microjet for Photoelectron Spectroscopy. *Nucl. Instrum. Methods Phys. Res., Sect. A* **2009**, *601*, 139–150.
- (17) Ludox SM-30 colloidal silica is an aqueous colloidal dispersion of 7 nm silica particles produced commercially by DuPont. The physical properties of the solution are well characterized and include the following: average particle diameter = 7 nm, specific surface area = 345 m<sup>2</sup>/g, and titratable Na<sub>2</sub>O = 0.56 wt % (for charge stabilization). The colloidal particles are amorphous in structure and nonporous. Ludox CL and Ludox HS-30 were used as stable aqueous colloidal suspensions of 12 and 22 nm silica, respectively. Further details are available from the DuPont product information brochure entitled “Ludox Colloidal Silica, Properties, Uses, Storage, and Handling”. This document is available free of charge, direct through DuPont or via one of its international distributors of Ludox.
- (18) Davoli, I.; Paris, E.; Stizza, S.; Benfatto, M.; Fanfoni, M.; Gargano, A.; Bianconi, A.; Seifert, F. Structure of Densified Vitreous Silica: Silicon and Oxygen XANES Spectra and Scattering Calculations. *Phys. Chem. Miner.* **1992**, *19*, 171–175.
- (19) Li, D.; Bancroft, G. M.; Kasrai, M.; Fleet, M. E.; Secco, R. A.; Feng, X. H.; Tan, K. H.; Yang, B. X. X-ray Absorption Spectroscopy of Silicon Dioxide (SiO<sub>2</sub>) Polymorphs — The Structural Characterization of Opal. *Am. Mineral.* **1994**, *79*, 622–632.
- (20) Wong, J.; Angell, C. A. *Glass Structure by Spectroscopy*; Marcel Dekker: New York, 1976.
- (21) Li, D.; Bancroft, G. M.; Kasrai, M.; Fleet, M. E.; Feng, X. H.; Tan, K. H. High Resolution Si K- and L<sub>2,3</sub>-Edge XANES of  $\alpha$ -Quartz and Stishovite. *Solid State Commun.* **1993**, *87*, 613–617.
- (22) Brown, M. A.; Seidel, R.; Thurmer, S.; Faubel, M.; Hemminger, J. C.; van Bokhoven, J. A.; Winter, B.; Sterrer, M. Electronic Structure of Sub-10 nm Colloidal Silica Nanoparticles Measured by In Situ

Photoelectron Spectroscopy at the Aqueous–Solid Interface. *Phys. Chem. Chem. Phys.* **2011**, *13*, 12720–12723.

(23) Metin, C. O.; Lake, L. W.; Miranda, C. R.; Nguyen, Q. P. Stability of Aqueous Silica Nanoparticle Dispersions. *J. Nanopart. Res.* **2011**, *13*, 839–850.

(24) Levelut, C.; Cabaret, D.; Benoit, M.; Jund, P.; Flank, A. M. Multiple Scattering Calculations of the XANES Si K-Edge in Amorphous Silica. *J. Non-Cryst. Solids* **2001**, *293*, 100–104.

(25) Okubo, T. Surface Tension of Structured Colloidal Suspensions of Polystyrene and Silica Spheres at the Air–Water Interface. *J. Colloid Interface Sci.* **1995**, *171*, 55–62.

(26) Iler, R. K. *The Chemistry of Silica: Solubility, Polymerization, Colloid and Surface Properties and Biochemistry of Silica*; Wiley: New York, 1979.